

Hot-carrier-mediated impact excitation of Er^{3+} ions in SiO_2 sensitized by Si Nanocrystals

Cite as: Appl. Phys. Lett. **113**, 031109 (2018); <https://doi.org/10.1063/1.5042013>

Submitted: 29 May 2018 . Accepted: 07 July 2018 . Published Online: 20 July 2018

A. Lesage,  D. Timmerman, D. M. Lebrun, Y. Fujiwara, and  T. Gregorkiewicz



View Online



Export Citation



CrossMark

ARTICLES YOU MAY BE INTERESTED IN

[Band alignment of \$\text{In}_2\text{O}_3/\beta\text{-Ga}_2\text{O}_3\$ interface determined by X-ray photoelectron spectroscopy](#)

Applied Physics Letters **113**, 031603 (2018); <https://doi.org/10.1063/1.5038615>

[Probing the free-carrier absorption in multi-layer black phosphorus](#)

Applied Physics Letters **113**, 031108 (2018); <https://doi.org/10.1063/1.5040963>

[Enhancement of the deep-level emission and its chemical origin in hexagonal boron nitride](#)

Applied Physics Letters **113**, 031903 (2018); <https://doi.org/10.1063/1.5038168>

 QBLOX



1 qubit

Shorten Setup Time

Auto-Calibration
More Qubits

Fully-integrated

Quantum Control Stacks
Ultrastable DC to 18.5 GHz
Synchronized <<1 ns
Ultralow noise



100s qubits

[visit our website >](#)

Hot-carrier-mediated impact excitation of Er^{3+} ions in SiO_2 sensitized by Si Nanocrystals

A. Lesage,¹ D. Timmerman,¹ D. M. Lebrun,² Y. Fujiwara,² and T. Gregorkiewicz^{1,2}

¹Van der Waals-Zeeman Institute, University of Amsterdam, Science Park 904, 1098 XH Amsterdam, The Netherlands

²Division of Materials and Manufacturing Science, Graduate School of Engineering, Osaka University, 2-1 Yamadaoka, Suita, Osaka 565-0871, Japan

(Received 29 May 2018; accepted 7 July 2018; published online 20 July 2018)

Past research has shown that indirect excitation of Er^{3+} ions in SiO_2 solid-state matrix with Si nanocrystals can be achieved by different pathways. Here, we investigate the impact excitation mechanisms in detail by means of time-resolved photoluminescence spectroscopy. We explicitly demonstrate that the free carrier impact excitation mechanism is activated as soon as the carriers obtain sufficient excess energy. The “hot” carriers with the above-threshold energy can be created upon optical pumping in two ways: either upon absorption of (i) a single photon with an energy exceeding a certain threshold $h\nu > E_{\text{th}}$ or (ii) following absorption of multiple photons of lower energy in a single nanocrystal, $h\nu < E_{\text{th}}$, followed by an Auger recombination of the generated multiple e-h pairs. In addition, we show that the impact excitation dynamics by hot carriers are similar, regardless of the mode in which they have been created. *Published by AIP Publishing.*

<https://doi.org/10.1063/1.5042013>

Featuring $1.5\ \mu\text{m}$ emission coincident with the absorption minimum of optical fibers, Er-doped materials are broadly explored for, and applied in, telecommunication networks. The emission arises from radiative transitions between J states of the incomplete 4f electron shell of Er^{3+} ions.¹ Due to the effective screening of the 4f shell by the complete outer 5s and 5p orbitals, the host has only a very limited influence on the energy structure of the Er^{3+} ions; consequently, a narrow emission band with a temperature invariant wavelength can be observed up to room temperature. However, transitions between the individual J states are only weakly allowed, yielding very long radiative lifetimes ($\sim\text{ms}$) and very small optical absorption cross-sections for resonant excitation.² Consequently, excitation of Er-doped insulating materials can only be achieved by resonant pumping with high-power tunable lasers, which is cumbersome and energy-inefficient. Past research revealed that the excitation cross-section of Er^{3+} ions in SiO_2 can be increased by up to 3 orders of magnitude by co-doping with Si nanocrystals (NCs). In contrast to Er, Si NCs feature a large absorption cross section over a wide energy range. Moreover, when in direct neighborhood of each other, a strong coupling appears between the Si NC and the Er^{3+} ions, leading to an effective sensitization of Er^{3+} emission.^{3–6} In this case, the Si NC absorbs a photon and, due to the relatively long excitation life time, it can transfer its energy non-radiatively to an Er^{3+} ion promoting it to one of its excited states. The sensitization effect of the $1.5\ \mu\text{m}$ Er-related emission^{4,7–9} opened perspectives for Er-doped SiO_2 with possible application for broad-band flash lamp pumped amplifiers and lasers for telecommunication networks, but also a wide range of other applications, such as laboratory-on-a-chip, optoelectronics, all Si lasers,¹⁰ and also future photovoltaics.^{11,12}

The sensitization process has been extensively investigated and modeled,^{13–15} but a full understanding hereof, and

thus optimization, remains challenging. It has been shown that only Er^{3+} ions in the vicinity of a Si NC can be indirectly excited via Si NCs, and those constitute a minor fraction of the total Er concentration. By dedicated experiments, it was revealed that in optimized materials only approximately 1% of the overall concentration of Er^{3+} could be indirectly excited via Si NCs. While later attempts slightly increased that percentage,¹⁶ it remained low, thus precluding realization of population inversion, and optical gain.¹⁷

The energy transfer between Si NC and Er^{3+} ions is a complex, multichannel process.^{5,18} Using a series of time-resolved PL experiments, PL excitation spectroscopy, and PL quantum yield determination, it has been shown that the non-resonant Er excitation processes proceed by two different energy transfer mechanisms. A “slow” one, involving the afore-mentioned non-radiative recombination of an e-h pair in a Si NC accompanied by energy transfer to a nearby Er^{3+} ion, is relatively well understood. A second “fast” mechanism takes place within $1\ \mu\text{s}$ after a pulsed excitation and has been related either to an intraband relaxation of a hot carrier in a Si NC, analogous to impact excitation by hot carriers in bulk semiconductors,^{12,19,20} or energy transfer via luminescence centers.²¹ While the luminescence center mediated transfer can always occur, the impact ionization path requires enough excess energy of the generated e-h pairs. Since the efficiency of the “fast” process can be much higher than that of the “slow” one, it has an interesting application potential.

Here, we examined the dynamics of Er emission sensitized by Si NCs under different excitation conditions. Two excitation photon energies were used, one below the threshold E_{th} , defined by the sum of the Si NC bandgap energy and that of the first excited state of Er^{3+} , and a second one larger than E_{th} . For both excitation photon energies, a wide range of pump fluences was employed. For the lowest pump

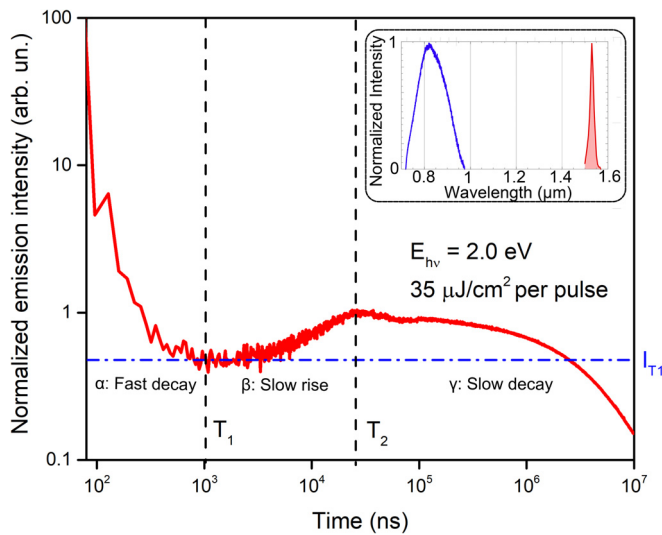


FIG. 1. Log-log plot of the typical PL dynamics measured at 1535 nm. There are 3 distinct stages: an initial fast decay with a time constant of a few tens of ns. This is followed by a slower rise and finally a slow decay with a time constant of 4 ms. The emission intensity is normalized at T_2 , the maximum of the concentration of excited Er^{3+} ions. The intensity at the minimum, I_{T1} , indicates the excited Er^{3+} concentration obtained by fast processes. The inset depicts the normalized emission spectra of the sample with the Si NC emission spectra around 920 nm (blue) and Er^{3+} emission around 1535 nm (red).

fluence, it was ensured that the average amount of absorbed photons per NC during a pulse²² was much smaller than 1, to ensure there are no multiple photon absorption events in a single NC during a pulse.

The samples used in this work consisted of a series of Er-doped SiO_2 with Si NCs layers prepared by radio-frequency co-sputtering. After deposition of a $2\ \mu\text{m}$ thick SiO_2 layer enriched with Si on a quartz substrate, they were annealed at 1200°C in N_2 atmosphere for 30 min to form Si NCs. The Er concentration was maintained at $2.7 \times 10^{19}\ \text{cm}^{-3}$. The concentration of Si NCs was determined to be $2.1 \times 10^{18}\ \text{cm}^{-3}$ with an average diameter of 3 nm. More details on the fabrication process and material characterization can be found in Ref. 7.

Time-dependent PL excitation spectroscopy was performed with an Optical Parametric Oscillator (OPO) system (Solar LS). The 3rd harmonic of a Nd:YAG laser (100 Hz, 5 ns pulsewidth) was used to pump a tunable OPO for

generation of the different photon energies. Detection was performed with a NIR photomultiplier tube (Hamamatsu R5509-73), combined with a multiscaler card to register events.

Figure 1 shows the different time regimes in the decay dynamics of $1.5\ \mu\text{m}$ emission sensitized by Si NCs, observed in time resolved PL over 5 orders of magnitude from ns to ms. In the first region (α), a fast decay can be observed and has a typical time constant of a few tens of ns. It has been suggested to be due to a combination of defect-related emission and a fast direct excitation of Er^{3+} ions competing with efficient non-radiative processes of energy back transfer from Er^{3+} to the NC core.^{21,23,24} The second region (β) shows a slower rise, indicating the energy transfer from Si NCs to Er by non-radiative recombination of the e-h pair. The time constant of this rise is determined by the combination of the energy transfer time and the relaxation time from the higher excited states to the 1st excited state of Er. The most important contribution to the latter process is that of the $^4I_{11/2}$ to $^4I_{13/2}$ excited state transition, with a time constant of $\sim 2.4\ \mu\text{s}$.²¹ Using this value and fitting the rise with rate equations describing the transfer, we find a value of $\sim 10\ \mu\text{s}$ for the energy transfer time. The last region (γ) depicts the normal decay of Er^{3+} ions and has a time constant of $\sim 4\ \text{ms}$. As there are no energy transfer processes taking place after all the NCs have transferred their energy, for the remainder of the manuscript, we focus on the first $35\ \mu\text{s}$ after the pump pulse. In order to make quantitative comparisons between the different decay kinetics, we set the maximum of the emission intensity around $t = 30\ \mu\text{s}$ (I_{T2}) to 1 and determine the value of the lowest part of the emission intensity at $t = 1\ \mu\text{s}$ to be I_{T1} , indicative for the Er concentration that is excited by processes faster than that by “slow” energy transfer, due to the non-radiative recombination of e-h pairs.

We have probed the PL dynamics by two excitation photon energies. The first one being $E_{\text{hv}} = 2\ \text{eV}$, below the threshold value, E_{th} , of $\sim 2.2\ \text{eV}$, determined by the sum of Er^{3+} 1st excited state and the NC bandgap energy. The second one above the threshold with a photon energy of $E_{\text{hv}} = 2.8\ \text{eV}$. In both cases, the excitation power was varied to probe the decay kinetics for different excited NCs concentration after the pulse. In Fig. 2(a), the values of I_{T1} are

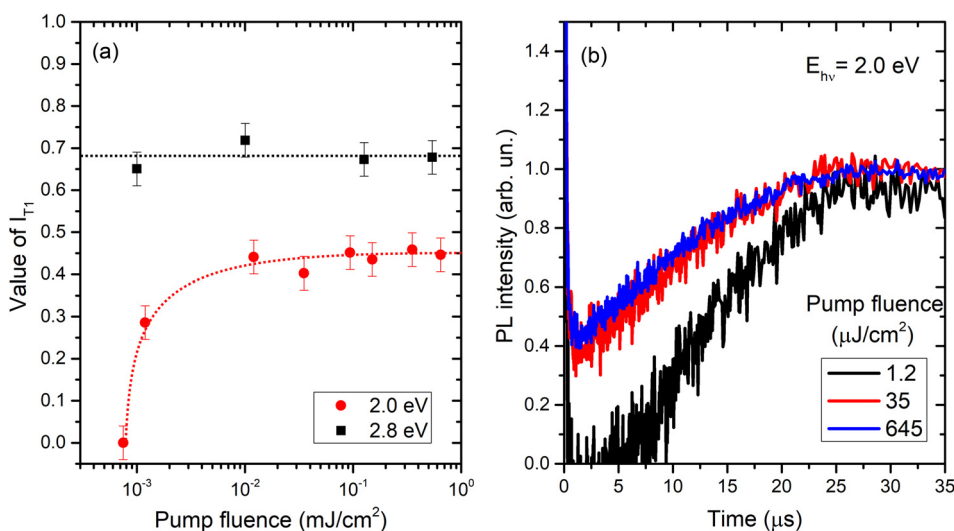


FIG. 2. (a) Values of I_{T1} as a function of pump fluence for the two excitation photon energies used in this study. The dashed lines serve as guide to the eyes. (b) Time-resolved PL intensity for 3 different values of the pump fluence for the first $35\ \mu\text{s}$ for an excitation photon energy of 2 eV.

determined as function of average number of absorbed photons per NC, as determined following the procedure described in Ref. 23. We note that I_{T1} is proportional to the population of Er ions that are excited via fast processes. We observe that for the case of $E_{h\nu} = 2.8$ eV, there is no change of I_{T1} for different excitation powers. The contribution of Er^{3+} ions excited by the fast process is about 70% of the total population of excited Er^{3+} ions, over the whole range from very low excitation flux up to very high. In contrast, for a photon energy of $E_{h\nu} = 2$ eV, the “fast” contribution goes down for small fluxes, and even completely disappears for the smallest excitation density. We note that the decay kinetics still show a fast ns component, but this does not give rise to any excited Er^{3+} ions which could be observed for longer times, and thus can be completely designated to “defect-related” emission. At larger values of the pump fluence at $E_{h\nu} = 2$ eV, the value of I_{T1} stabilizes at approximately 45% of the total excited Er^{3+} population.

From above results, we can draw the following conclusions: For a low photon fluence at $E_{h\nu} = 2$ eV, there is only one excitation mechanism taking place, which is the slow non-radiative recombination of excitons in Si NCs exciting Er^{3+} ions into a higher state, which is then followed by subsequent relaxation to the first excited state. This is distinctively different for the cases where either a high fluence or a larger photon energy $E_{h\nu} = 2.8$ eV are applied. Under both of these pumping conditions, the Er-related PL dynamics is similar and considerably different to that recorded while pumping at $E_{h\nu} = 2$ eV at low flux. In the case of a large photon energy, there is, next to the slow excitation pathway, also the fast additional excitation mechanism active. This takes place on a short timescale and is obscured in the PL dynamics by the convolution of Er^{3+} emission with a fast defect-related band at the same detection wavelength. The proportion of Er^{3+} ions excited by the fast process can be distinguished by I_{T1} , as the defect related emission does not contribute after $1 \mu\text{s}$, and the excited Er^{3+} ions have not decayed yet. For a larger pump fluence at $E_{h\nu} = 2$ eV, a different process can occur giving rise to a similar behavior. This is likely a result of multiple photon absorption in a single NC, followed by an Auger process, in which one e-h pair recombines and transfers its energy to one of the other carriers, effectively creating a “hot” carrier with excess energy, similar as obtained by large energy photon absorption. A schematic of the different excitation conditions and energy transfer processes is depicted in Fig. 3.

When we compare our results with those of Refs. 21 and 23, we can see that for the conditions illustrated in Figs. 3(b) and 3(c), we can draw similar conclusions about the relative contribution of the fast and slow process to the excitation of Er^{3+} . However, while in those cases the fast excitation was determined to be mediated by defects/luminescence centers, we explicitly show that this process does not occur in high temperature annealed samples. In this case, it is the excess carrier energy, either created by large photon energy or large absorbed photon fluxes followed by an Auger process, which is the physical mechanism behind the fast excitation process. We believe that the high temperature annealing creates high quality Si nanocrystals and removes the defects which can provide a fast excitation channel for Er^{3+} ions in matrices of

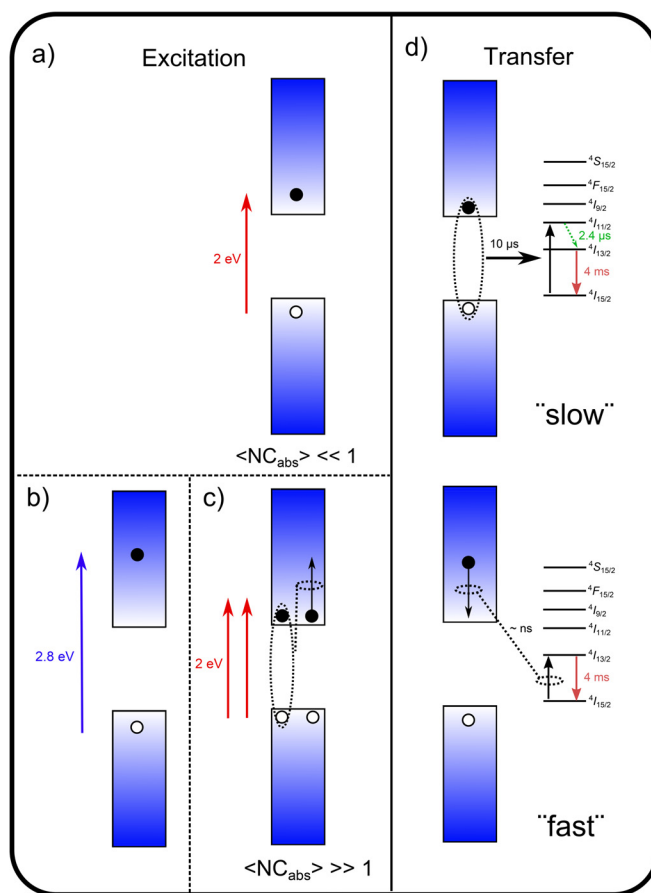


FIG. 3. Schematics of the different excitation conditions and energy transfer processes from Si NCs to Er^{3+} ions. (a) Low pump fluence and small photon energy, a single low energy e-h pair is created in a Si NC. (b) Absorption of a high energy photon leads to generation of high energy e-h pair. (c) Absorption of multiple small photon energy photons at large pump flux leads to generation of multiple e-h pairs in single NCs. Subsequently, recombination of one e-h pair transfers its energy in an Auger process (indicated by the dotted lines), leaving behind a single high energy e-h pair. (d) Energy transfer to Si NCs to Er ions. The slow process takes place upon recombination of a low energy e-h pair, with a transfer time of $10 \mu\text{s}$, exciting Er^{3+} ions to a higher excited state. A second “fast” process can only occur for the conditions indicated in (b) and (c). Excess energy of a “hot” carrier is transferred by means of impact ionization, exciting Er^{3+} ions directly into the $4I_{13/2}$ state.

lesser crystalline quality. Also, because of the longer carrier lifetimes which accompany the good crystallinity, the Auger process becomes possible and gives rise to the hot carrier mediated Er^{3+} excitation process. Although it is difficult to pinpoint the exact reason for the difference in the value of I_{T1} for both photon energies at high flux, there are some comments we can make with might be related to this. First, there might be a difference in the subset of excited NCs due to the difference in absorption cross-section. Second, in the case of 2 eV excitation, we might not have reached the saturation yet, so a subset of Si NCs is still only singly excited and not contributing to I_{T1} , leading to a smaller value. This effect will be additionally enhanced by the inhomogeneity of the laser field in the excitation spot.

We have used time-resolved PL to probe the energy transfer dynamics of Si NCs to Er^{3+} ions in Er-doped Si rich SiO_2 films. By using two excitation energies, one below the threshold value of Si NC bandgap and 1st excited state of Er^{3+} , and the other one above, we demonstrated that at low pump fluence, the fast (sub μs) excitation process does not

take place below the threshold pump photon energy. This explicitly demonstrates that there is no “defect” mediated direct excitation process active in our materials.

Furthermore, we demonstrate that an additional excitation pathway by hot-carrier-mediated impact becomes activated as soon as there are carriers available with sufficiently large excess energy. These can be created by absorption of above energy threshold photons, or by the absorption of multiple sub-threshold photons in a single NC followed by an Auger process. In both cases, the decay kinetics are nearly identical and the contribution to the total excited Er population is for the largest part a result of the hot carrier mediated pathway, which is responsible for 45%–70% of the total population of excited Er³⁺ ions. These results show the importance of choosing the right excitation conditions for this system, and offer a possible pathway for reaching population inversion.

A.L., D.T., and T.G. acknowledge the Netherlands Organization of Scientific Research (NWO) for financial support. This work was supported in part by the International Joint Research Promotion Program of Osaka University.

¹M. Fujii, S. Hayashi, and K. Yamamoto, *J. Nanopart. Res.* **1**, 83 (1999).

²P. G. Kik and A. Polman, *Mater. Sci. Eng. B* **81**, 3 (2001).

³A. J. Kenyon, P. F. Trwoga, M. Federighi, and C. W. Pitt, *J. Phys.: Condens. Matter* **6**, L319 (1994).

⁴J. H. Shin, S.-Y. Seo, S. Kim, and S. G. Bishop, *Appl. Phys. Lett.* **76**, 1999 (2000).

⁵P. G. Kik, M. L. Brongersma, and A. Polman, *Appl. Phys. Lett.* **76**, 2325 (2000).

⁶L. A. Padilha, J. T. Stewart, R. L. Sandberg, W. K. Bae, W. K. Koh, J. M. Pietryga, and V. I. Klimov, *Acc. Chem. Res.* **46**, 1261 (2013).

⁷A. Dorofeev, E. Bachilo, V. Bondarenko, N. Gaponenko, N. Kazuchits, A. Leshok, G. Troyanova, N. Vorozov, V. Borisenko, H. Gnaser, W. Bock, P. Becker, and H. Oechsner, *Solid Films* **276**, 171 (1996).

⁸M. Fujii, M. Yoshida, Y. Kanzawa, S. Hayashi, and K. Yamamoto, *Appl. Phys. Lett.* **71**, 1198 (1997).

⁹G. Franzò, D. Pacifici, V. Vinciguerra, F. Priolo, and F. Iacona, *Appl. Phys. Lett.* **76**, 2167 (2000).

¹⁰R. Soref, *IEEE J. Sel. Top. Quantum Electron.* **12**, 1678 (2006).

¹¹F. Priolo, T. Gregorkiewicz, M. Galli, and T. F. Krauss, *Nat. Nanotechnol.* **9**, 19 (2014).

¹²S. Saeed, E. M. de Jong, K. Dohnalova, and T. Gregorkiewicz, *Nat. Commun.* **5**, 4665 (2014).

¹³A. Kozanecki, B. J. Sealy, K. Homewood, S. Ledain, W. Jantsch, and D. Kuritsyn, *Mater. Sci. Eng. B* **81**, 23 (2001).

¹⁴A. J. Kenyon, *Semicond. Sci. Technol.* **20**, R65 (2005).

¹⁵A. A. Prokofiev, A. S. Moskalenko, and I. N. Yassievich, *Mater. Sci. Eng. B* **146**, 121 (2008).

¹⁶L. Khomenkova, F. Gourbilleau, J. Cardin, and R. Rizk, *Physica E* **41**, 1048 (2009).

¹⁷M. Wojdak, M. Klik, M. Forcales, O. B. Gusev, T. Gregorkiewicz, D. Pacifici, G. Franzò, F. Priolo, and F. Iacona, *Phys. Rev. B: Condens. Matter Mater. Phys.* **69**, 233315 (2004).

¹⁸F. Priolo, G. Franzò, D. Pacifici, V. Vinciguerra, F. Iacona, and A. Irrera, *J. Appl. Phys.* **89**, 264 (2001).

¹⁹I. Izeddin, A. S. Moskalenko, I. N. Yassievich, M. Fujii, and T. Gregorkiewicz, *Phys. Rev. Lett.* **97**, 207401 (2006).

²⁰I. Izeddin, D. Timmerman, T. Gregorkiewicz, A. S. Moskalenko, A. A. Prokofiev, I. N. Yassievich, and M. Fujii, *Phys. Rev. B: Condens. Matter Mater. Phys.* **78**, 035327 (2008).

²¹O. Savchyn, F. R. Ruhge, P. G. Kik, R. M. Todi, K. R. Coffey, H. Nukala, and H. Heinrich, *Phys. Rev. B* **76**, 195419 (2007).

²²D. Timmerman, I. Izeddin, and T. Gregorkiewicz, *Phys. Status Solidi A* **207**, 183 (2010).

²³N. Prtljaga, D. Navarro-Urrios, A. Pitanti, F. Ferrarese-Lupi, B. Garrido, and L. Pavesi, *J. Appl. Phys.* **111**, 094314 (2012).

²⁴D. Timmerman, I. Izeddin, P. Stallinga, I. N. Yassievich, and T. Gregorkiewicz, *Nat. Photonics* **2**, 105 (2008).